Optimization of an intracavity Q-switched solid-state second order Raman laser

Laser Phys. 27 (2017) 015405 (7pp) doi:10.1088/1555-6611/27/1/015405

Optimization of an intracavity Q-switched solid-state second order Raman laser

Zhiqiong Chen[1,2], Xihong Fu[1], Hangyu Peng[1], Jun Zhang[1], Li Qin[1] and Yongqiang Ning[1]

[1] Changchun Institute of Optics, Fine Mechanics and Physics, Chinese Academy of Sciences, Changchun 130033, People's Republic of China

[2] University of Chinese Academy of Sciences, Beijing 100039, People's Republic of China

E-mail: fuxh@ciomp.ac.cn

Received 19 August 2016, revised 24 October 2016
Accepted for publication 28 October 2016
Published 7 December 2016

Abstract

In this paper, the model of an intracavity Q-switched second order Raman laser is established, the characteristics of the output 2nd Stokes are simulated. The dynamic balance mechanism among intracavity conversion rates of stimulated emission, first order Raman and second order Raman is obtained. Finally, optimization solutions for increasing output 2nd Stokes pulse energy are proposed.

Keywords: 2nd Stokes, second order Raman, pulse energy, balance mechanism, coupled cavity

(Some figures may appear in colour only in the online journal)

1. Introduction

Stimulated Raman scattering is an important nonlinear optical frequency conversion method. It can not only fill up the spectral region that has not been realized by the traditional laser, but also has the effect of beam clean-up. Therefore, the Raman laser is widely used in communications, medical, military and other fields. Second order Raman scattering has a great advantage in obtaining an infrared laser, especially in the mid infrared range [1]. With the development of CVD diamond [2–5] and other Raman materials with excellent thermal conductivity, it is possible to obtain high pulse energy 2nd Stokes.

In recent years, several second order intracavity Raman lasers have been reported. Chen [6] used a double-end diffusion-bonded Nd:YVO_4 composite crystal as the gain and Raman medium, obtained 2nd Stokes at 1313 nm with 2.34 W output, corresponding pulse energy of 58 μJ, the conversion efficiency of 16%. Du [7] obtained 2nd Stokes output at 1314 nm with 40 μJ pulse energy by a Q-switched composite YVO_4/Nd:YVO_4/YVO_4 crystal self-Raman laser, corresponding conversion efficiency of 4.1%. As a contrast, Zhao [8] reported an intracavity first order Raman laser based on $BaWO_4$, the pulse energy of the 1st Stokes laser was 0.31 mJ. And an external cavity 2nd Stokes Raman laser at 1485 nm with 370 μJ pulse energy has been reported by Aaron [9]. Compared with the first order Raman laser and external cavity Raman laser, as reported previously, the intracavity second order Raman laser could not convert pump-power into 2nd Stokes efficiently, and this results in low output pulse energy. Optimization solutions for maximizing 2nd Stokes output pulse energy need to be proposed.

In theory, many rate equation models were established for the maximization of 1st Stokes output pulse energy [10–12]. Factors such as transit time of the ultrasonic wave [13], spatial and spectral effects [14], switching off/on times of the actively Q-switch [15] were studied to improve the performance of the first order Raman laser. But theoretical research about the second order Raman laser is rare. In 2011, Sabella [16] increased the conversion efficiency of the external cavity second order Raman laser with low output coupling reflectivity, and pointed out that balancing conversion rates of intracavity stimulated emission, first order Raman and second order Raman scattering can improve the pulse energy, but the balance mechanism is not clear.

In this paper, the balance mechanism of intracavity conversion rates among stimulated emission, first order Raman and second order Raman was explained for the first time, as far as we know. Based on that, cavity parameters for high pulse

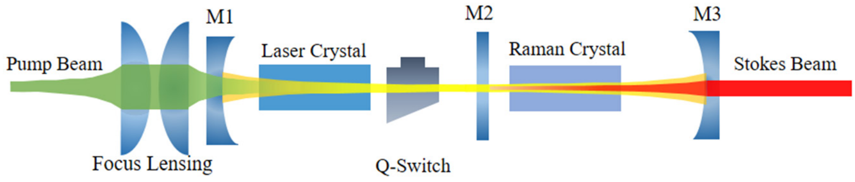

Figure 1. Schematics of the intracavity Q-switched Raman laser.

energy 2nd Stokes output were optimized. Firstly, a numerical model for the intracavity Q-switched second order Raman laser was implemented. Then the rate equations were solved and 2nd Stokes output characteristics were simulated through adjusting beam radius, cavity length and transmission of the insert coupler. Finally, numerical results were given and discussed.

2. Theory

Schematics of the intracavity second order Raman laser is shown in figure 1. Mirrors $M1$–$M3$ form a fundamental laser cavity, while $M2$–$M3$ form a Raman cavity (for both 1st and 2nd Stokes). We choose Nd:YVO_4 as the gain medium, and CVD-diamond as the Raman medium, which has a high Raman gain coefficient ($10\,\mathrm{cm\ GW^{-1}}$@$1064\,\mathrm{nm}$), large Raman shift ($1332.3\,\mathrm{cm^{-1}}$), excellent thermal conductivity ($2000\ \mathrm{W\ mK^{-1}}$) and wide transmittance range ($>0.23\,\mu$m) [17].

The intracavity photons are Gaussian spatial distribution when the fundamental and Raman beam are assumed to be TEM_{00} mode. And considering the variation of the beam size along the axis, the expression of intracavity photon densities $\phi(r,t)$ can be given as follows:

$$\begin{cases} \phi_1(r,t) = \phi_1(0,t)\exp\left(\dfrac{-2r^2}{w_1^2}\right) \\ \phi_{s1}(r,t) = \phi_{s1}(0,t)\exp\left(\dfrac{-2r^2}{w_{s1}^2}\right) \\ \phi_{s2}(r,t) = \phi_{s2}(0,t)\exp\left(\dfrac{-2r^2}{w_{s2}^2}\right) \end{cases} \tag{1}$$

where ϕ_1 is photon density and w_1 is the beam radius of fundamental photon at the gain medium. Fundamental photon densities ϕ_r and beam radius w_r at the Raman medium can be obtained from the following relation: $\phi_1(0,t)\times w_1^2 = \phi_r(0,t)\times w_r^2$; ϕ_{s1}, ϕ_{s2} are photon densities, w_{s1}, w_{s2} are the beam radius of 1st and 2nd Stokes at the Raman medium, respectively.

Considering the second order stimulated Raman scattering process, ignoring the third and higher order terms, regardless of spontaneous emission, the rate equations of the intracavity second order Q-switched Raman laser can be established as follows [18]:

$$\begin{cases} \displaystyle\int_0^\infty \frac{\mathrm{d}\phi_1(r,t)}{\mathrm{d}t}\cdot 2\pi r\mathrm{d}r = \frac{1}{t_{\mathrm{rl}}}\cdot\int_0^\infty 2\sigma n(r,t)\phi_1(r,t)l_1\cdot 2\pi r\mathrm{d}r - \frac{1}{t_l}\int_0^\infty \phi_l(r,t)\cdot 2\pi r\mathrm{d}r \\ \qquad\displaystyle -\frac{1}{t_{\mathrm{rs}}}\cdot\int_0^\infty 2g_s l_s ch\nu_{s1}\phi_{s1}(r,t)\phi_1(r,t)\frac{w_1^2}{w_r^2}\cdot 2\pi r\mathrm{d}r \\ \displaystyle\int_0^\infty \frac{\mathrm{d}\phi_{s1}(r,t)}{\mathrm{d}t}\cdot 2\pi r\mathrm{d}r = \frac{1}{t_{\mathrm{rs}}}\cdot\int_0^\infty 2g_s l_s ch\nu_{s1}\phi_{s1}(r,t)\phi_1(r,t)\frac{w_1^2}{w_r^2}\cdot 2\pi r\mathrm{d}r \\ \qquad\displaystyle -\frac{1}{t_{\mathrm{rs}}}\cdot\int_0^\infty 2g_s l_s ch\nu_{s2}\phi_{s2}(r,t)\phi_{s1}(r,t)\cdot 2\pi r\mathrm{d}r \\ \qquad\displaystyle -\frac{1}{t_{s1}}\int_0^\infty \phi_{s1}(r,t)\cdot 2\pi r\mathrm{d}r + k_{\mathrm{sr}}\int_0^\infty \phi_1(r,t)\frac{w_1^2}{w_r^2}\cdot 2\pi r\mathrm{d}r \\ \displaystyle\int_0^\infty \frac{\mathrm{d}\phi_{s2}(r,t)}{\mathrm{d}t}\cdot 2\pi r\mathrm{d}r = \frac{1}{t_{\mathrm{rs}}}\cdot\int_0^\infty 2g_s l_s ch\nu_{s2}\phi_{s2}(r,t)\phi_{s1}(r,t)\cdot 2\pi r\mathrm{d}r \\ \qquad\displaystyle -\frac{1}{t_{s2}}\int_0^\infty \phi_{s2}(r,t)\cdot 2\pi r\mathrm{d}r + k_{\mathrm{sr}}\int_0^\infty \phi_{s1}(r,t)\cdot 2\pi r\mathrm{d}r \\ \displaystyle\int_0^\infty \frac{\mathrm{d}n(r,t)}{\mathrm{d}t}\cdot 2\pi r\mathrm{d}r = \int_0^\infty -\gamma\sigma c n(r,t)\phi_{\mathrm{L}}(r,t)\cdot 2\pi r\mathrm{d}r \\ \qquad\displaystyle -\int_0^\infty \frac{n(r,t)}{\tau_{\mathrm{sp}}}\cdot 2\pi r\mathrm{d}r + p_{\mathrm{in}} \end{cases} \tag{2}$$

where l_{cl}, l_{cs} are fundamental and Raman cavity length; population inversion accumulating rate $p_{\mathrm{in}} = \frac{P_{\mathrm{abs}}}{h\nu l_1 \pi w_p^2}$; t_{rl}, t_{rs} are the round trip time of fundamental laser and Stokes, $t_r = \frac{2l_c}{c}$; t_1, t_{s1}, t_{s2} are the photon lifetime of fundamental laser, 1st and 2nd Stokes, $t = \frac{t_r}{\ln\left(\frac{1}{R_1 R_2}\right) + L_{1,s} + L_Q}$; R_1, R_2 are reflectivity of input and output coupler; L_1, L_s is the loss of cavity for fundamental laser and Stokes; L_Q is the AO Q-switch loss, according to Dashkevich [15], it can be calculated as (3).

$$L_Q = \begin{cases} \dfrac{A}{2}\left[\cos^2\left(\dfrac{t-t_0}{t_{\mathrm{fall}}}\cdot\pi\right)+1\right] & t_0 < t < t_0 + t_{\mathrm{fall}} \\ 0 & t_0 + t_{\mathrm{fall}} < t \end{cases} \tag{3}$$

where $A = \max\mathrm{loss} = -\ln(T_{\mathrm{on}})$ is the highest loss of the laser (Stokes) beam in the AO Q-switch, T_{on} is the transmittance of the AO Q-switch in the 'on' condition, t_{fall} is the fall time of the ultrasound wave in the AO Q-switch.

It is reasonable to assume that the population inversion density $n(r,t)$ can be expressed as follows [19]:

$$n(r,t) = n(0,t)\exp\left(\frac{-2r^2}{w_p^2}\right). \tag{4}$$

Substituting (1), (4) into (2), yields:

$$\begin{cases} \frac{\mathrm{d}\phi_{\mathrm{l}}(0,t)}{\mathrm{d}t} = \frac{1}{t_{\mathrm{rl}}}\cdot 2\sigma n(0,t)\phi_{\mathrm{l}}(0,t)l_{\mathrm{l}}\frac{w_{\mathrm{p}}^2}{(w_{\mathrm{p}}^2+w_{\mathrm{l}}^2)} - \frac{1}{t_{\mathrm{rs}}}\cdot 2g_{\mathrm{s1}}l_{\mathrm{s}}ch\nu_{\mathrm{s1}} \\ \qquad \times\ \phi_{\mathrm{s1}}(0,t)\phi_{\mathrm{l}}(0,t)\frac{w_{\mathrm{l}}^2}{w_{\mathrm{r}}^2}\frac{w_{\mathrm{s1}}^2}{(w_{\mathrm{s1}}^2+w_{\mathrm{l}}^2)} - \frac{1}{t_{\mathrm{l}}}\cdot\phi_{\mathrm{l}}(0,t) \\ \frac{\mathrm{d}\phi_{\mathrm{s1}}(0,t)}{\mathrm{d}t} = \frac{1}{t_{\mathrm{rs}}}\cdot 2g_{\mathrm{s1}}l_{\mathrm{s}}ch\nu_{\mathrm{s1}}\phi_{\mathrm{s1}}(0,t)\phi_{\mathrm{l}}(0,t)\frac{w_{\mathrm{l}}^2}{w_{\mathrm{r}}^2}\frac{w_{\mathrm{l}}^2}{(w_{\mathrm{s1}}^2+w_{\mathrm{l}}^2)} \\ \qquad -\frac{1}{t_{\mathrm{rs}}}\cdot 2g_{\mathrm{s2}}l_{\mathrm{s}}ch\nu_{\mathrm{s2}}\phi_{\mathrm{s2}}(0,t)\phi_{\mathrm{s1}}(0,t)\frac{w_{\mathrm{s2}}^2}{(w_{\mathrm{s1}}^2+w_{\mathrm{s2}}^2)} \\ \qquad -\frac{1}{t_{\mathrm{s1}}}\phi_{\mathrm{s1}}(0,t) + k_{\mathrm{sr}}\phi_{\mathrm{l}}(0,t)\frac{w_{\mathrm{l}}^2}{w_{\mathrm{r}}^2}\frac{w_{\mathrm{l}}^2}{w_{\mathrm{s1}}^2} \\ \frac{\mathrm{d}\phi_{\mathrm{s2}}(0,t)}{\mathrm{d}t} = \frac{1}{t_{\mathrm{rs}}}\cdot 2g_{\mathrm{s2}}l_{\mathrm{s}}ch\nu_{\mathrm{s2}}\phi_{\mathrm{s2}}(0,t)\phi_{\mathrm{s1}}(0,t)\frac{w_{\mathrm{s1}}^2}{(w_{\mathrm{s1}}^2+w_{\mathrm{s2}}^2)} \\ \qquad -\frac{1}{t_{\mathrm{s2}}}\phi_{\mathrm{s2}}(0,t) + k_{\mathrm{s}}\phi_{\mathrm{s1}}(0,t)\frac{w_{\mathrm{s1}}^2}{w_{\mathrm{s2}}^2} \\ \frac{\mathrm{d}n(0,t)}{\mathrm{d}t} = -\gamma\sigma cn(0,t)\phi_{\mathrm{L}}(0,t)\frac{w_{\mathrm{l}}^2}{(w_{\mathrm{p}}^2+w_{\mathrm{l}}^2)} - \frac{n(0,t)}{\tau_{\mathrm{sp}}} + p_{\mathrm{in}}\frac{2}{\pi w_{\mathrm{p}}^2} \end{cases} \tag{5}$$

The pulse energy can be expressed as follows according to the theory presented by Degnan [20]:

$$E_{\mathrm{s}} = \frac{\pi\omega_{\mathrm{s}}^2 ch\nu_{\mathrm{s}}\ln(1/R_{\mathrm{s}})}{4}\int\varphi_{\mathrm{s}}(0,t)\mathrm{d}t. \tag{6}$$

3. Results and discussion

According to the rate equation (4), intracavity conversion rates of stimulated radiation, first order and second order Raman are strongly influenced by the photon density distribution ϕ_{l}, ϕ_{s1}, ϕ_{s2} and round trip time t_{rl}, t_{rs}. Photon density can be changed by adjusting the beam radius, while round trip time of photons can be changed by adjusting the cavity length effectively. Thus, in order to balance the conversion rate, we start from optimizing the beam radius and cavity length. Besides, we use $M2$ to form the Raman cavity in the fundamental laser cavity. The 'coupled cavity' for the fundamental laser is formed by $M1$–$M2$–$M3$ when the high transmission of $M2$ is changed to be partially transmitting at fundamental laser wavelength. The coupled cavity can redistribute the fundamental photons density. Therefore, it is also analyzed for the purpose of increasing the output pulse energy.

The rate equations were solved numerically by the method of Runge–Kutta using Matlab. Parameters of media and laser cavity used in rate equation calculations are shown in table 1.

3.1. Optimazation of Raman beam radius

Intracavity photon densities can be changed by adjusting the beam radius directly. Figure 2 shows the pulse shape of intracavity fundamental photons, intracavity 1st Stokes and output 2nd Stokes at different Raman beam radius. If the Stokes beam radius is small (figure 2(a)), 1st Stokes and 2nd Stokes have large photon density. Short pulse build-up time and steep rise-time of 2nd Stokes indicate that the second order Raman scattering is strong. It makes 1st Stokes convert to 2nd Stokes rapidly. However, the lower density of 1st Stokes photons reduces the first order Raman scattering, and the pulse build-up time becomes longer. Because fundamental photons will be consumed a lot, the rest of the fundamental photons could not be converted to 1st Stokes fully. In contrast, if the Stokes beam radius is large (figure 2(c)), long pulse build-up time and slow rise-time of 2nd Stokes indicate that the second order Raman scattering is weak. It will waste part of 1st Stokes which does not convert to 2nd Stokes in a timely manner.

Table 1. Parameters of media and laser cavity used in rate equation calculations.

Designation	Symbol	Value
Stimulated-emission cross-section (cm^2)	σ	15.6×10^{-18} [21]
Fundamental wavelength (nm)	λ	1064
1st Stokes wavelength (nm)	λ_{s1}	1240
2nd Stokes wavelength (nm)	λ_{s2}	1485
Raman shift (cm^{-1})	$\Delta\lambda$	1332.3 [17]
1st Stokes Raman gain coefficient (cm GW^{-1})	g_{s1}	10 [17]
2nd Stokes Raman gain coefficient (cm GW^{-1})	g_{s2}	7.6 [22]
Raman cavity insert loss	L_{s}	0.08
Fundamental cavity insert loss	L_{l}	0.05
Spontaneous Raman scattering coefficient (/s)	K_{sr}	10^{-3}
Pump power (W)	P_{abs}	10
Active medium length (mm)	l_{l}	10
Raman crystal length (mm)	l_{r}	6
Pump waist radius (μm)	w_{p}	200
Fundamental beam waist (μm)	w_{l}	160
$M1$–$M2$ (cm)	—	10
Output coupler	T_{OC}	15%
Repetition (Hz)	F	50
Lifetime of fundamental photons(μm)	t_{l}	115

Figure 3 shows the variation of pulse energy with the Raman beam radius when the fundamental beam radius is 160 μm at Raman media. If the Stokes beam radius has optimum size (50 μm, figure 2(b)), 1st Stokes can make the best use of fundamental photons and convert to 2nd Stokes entirely. In other words, the optimized Stokes beam radius increases the output pulse energy through balancing the second order Raman with first order Raman conversion rate.

3.2. Optimazation of cavity length

Adjusting the Raman cavity ($M2$–$M3$) length can change the round-trip time of Stokes photons effectively (when the cavity becomes longer, we should decrease the $M2$, $M3$ radius of curvature to maintain the beam waist experimentally). The shorter the round trip time, the stronger first

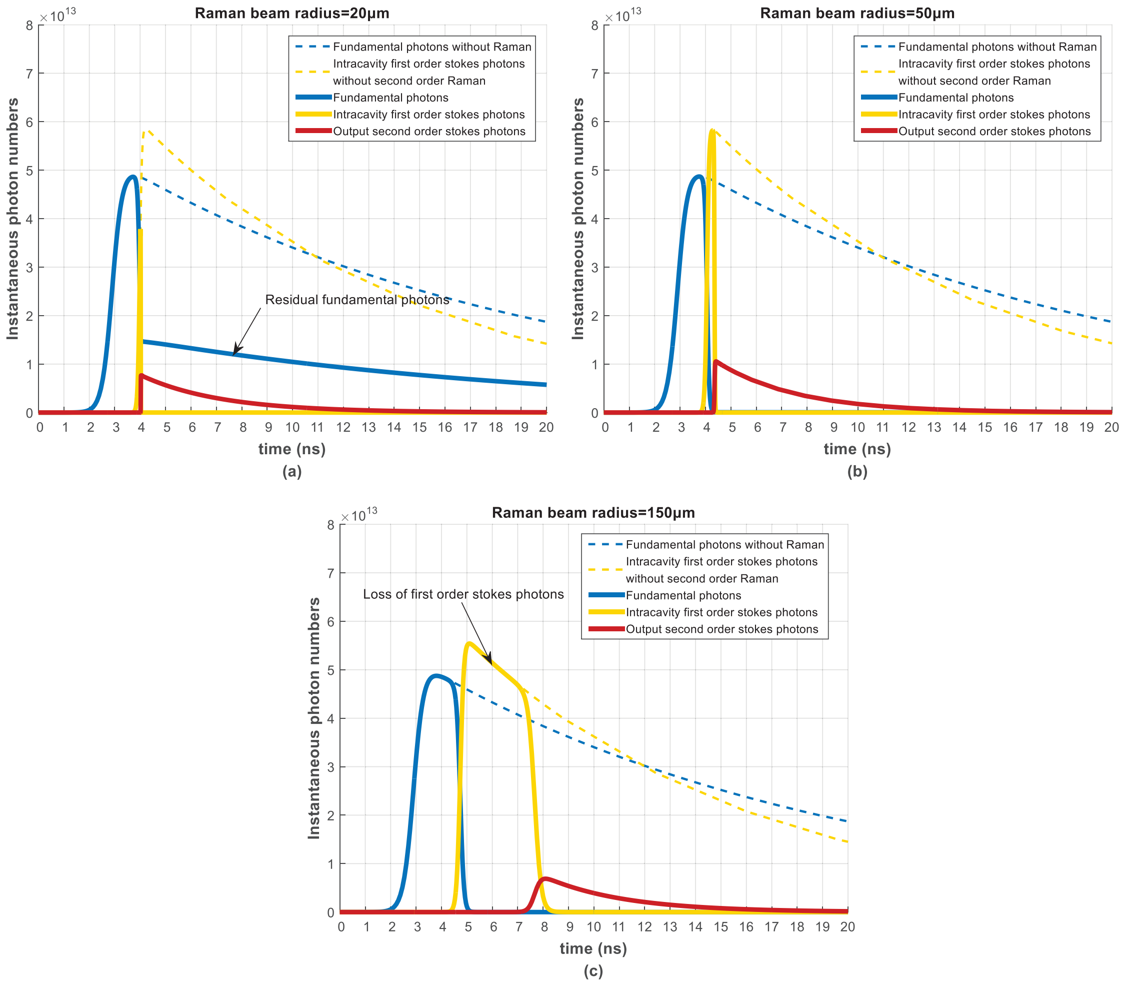

Figure 2. Pulse shape of intracavity fundamental photons, intracavity 1st Stokes and output 2nd Stokes at different Raman beam radii: (a) 20 μm; (b) 50 μm; (c) 150 μm.

order Raman, and the faster fundamental photons convert to 1st Stokes. As shown in figure 4(a), if the Raman cavity is small (5 cm), the short pulse build-up time and steep rise-time of 1st Stokes indicate that the first order Raman scattering is strong. And if the fundamental photon converts to 1st Stokes rapidly, the low density of fundamental photons reduces the intensity of stimulated radiation in return, this leads to the slow pulse build-up. On the occasion that the population inversion remains too much, a second pulse will generate. Because of the wastage and second pulse, population inversion could not convert to fundamental photons fully. In contrast, if the Raman cavity is long (figure 4(c)), build-up time and rise time of 1st Stokes pulse are slow, which indicates the first order Raman scattering is weak. It will waste part of the fundamental photons which do not convert to 1st Stokes quickly.

Figure 5 shows the variation of pulse energy with the cavity length, the optimum Raman cavity length is 10 cm (figure 4(b)) on the condition that the Stokes beam radius is 50 μm. Fundamental photons can make the best use of population inversion and convert to 1st Stokes entirely. In other words, the optimized Raman cavity length increases the output pulse energy through balancing the stimulated emission with the first order Raman conversion rate.

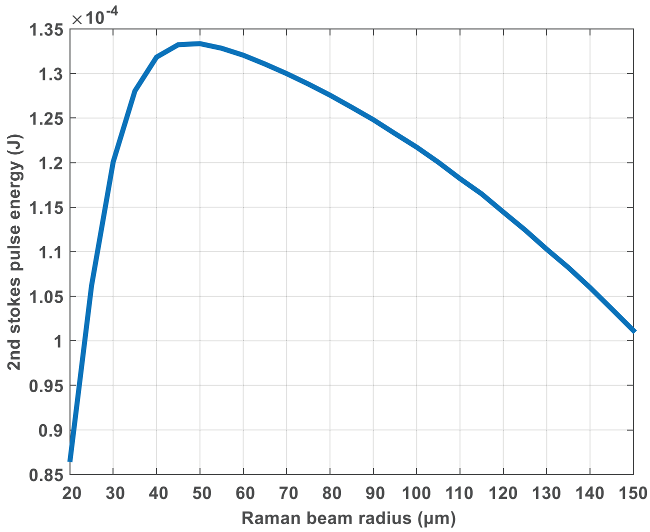

Figure 3. The variation of pulse energy with the Raman beam radius.

3.3. Optimization of insert coupler transmittance

As said above, we replace the mirror $M2$ (high transmitting at fundamental laser wavelength) with one that has partial transmission. With the mirror, the fundamental photon densities at

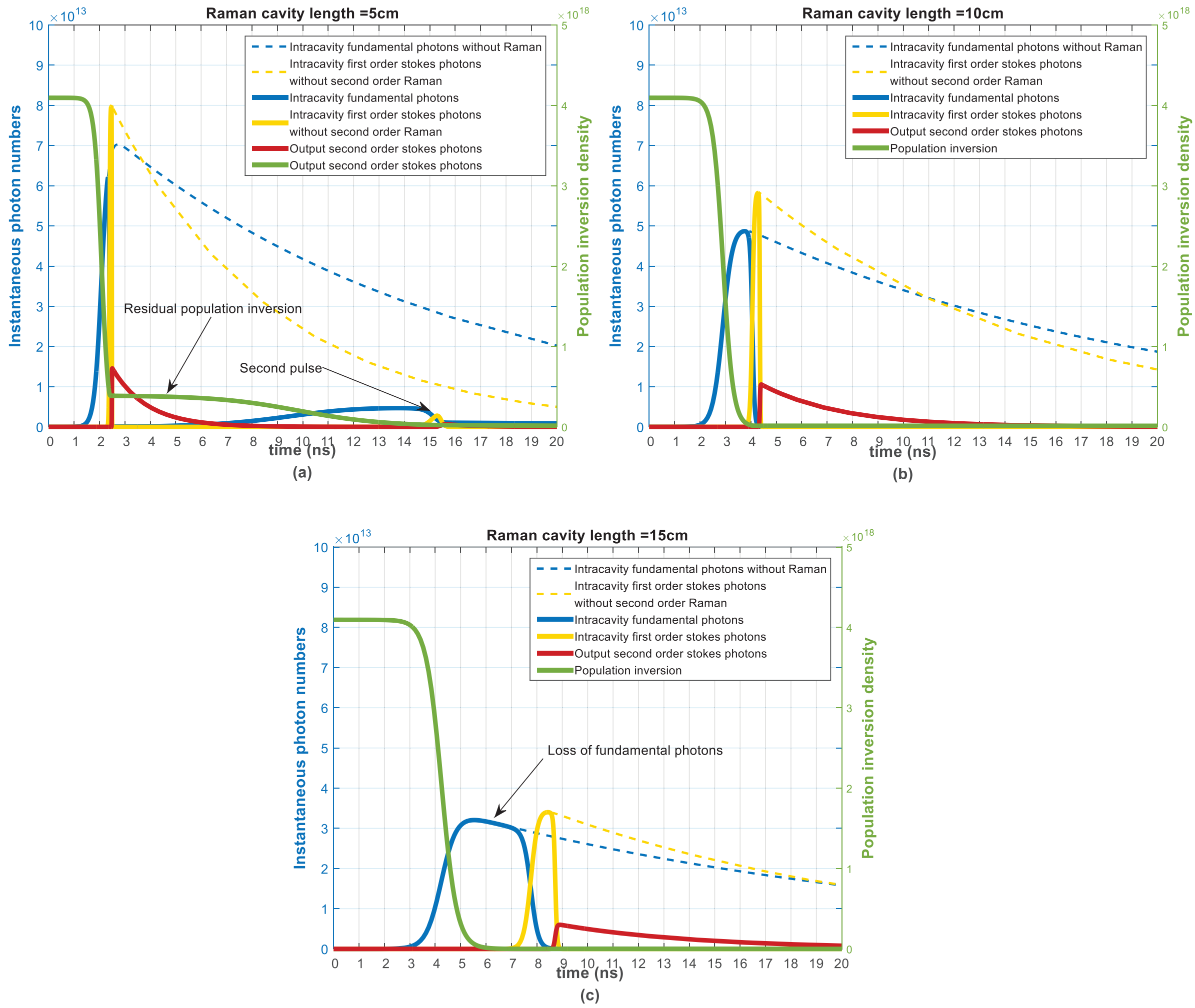

Figure 4. Pulse shape of intracavity fundamental photons, intracavity 1st Stokes and output 2nd Stokes at different cavity lengths: (a) 5 cm; (b) 10 cm; (c) 15 cm.

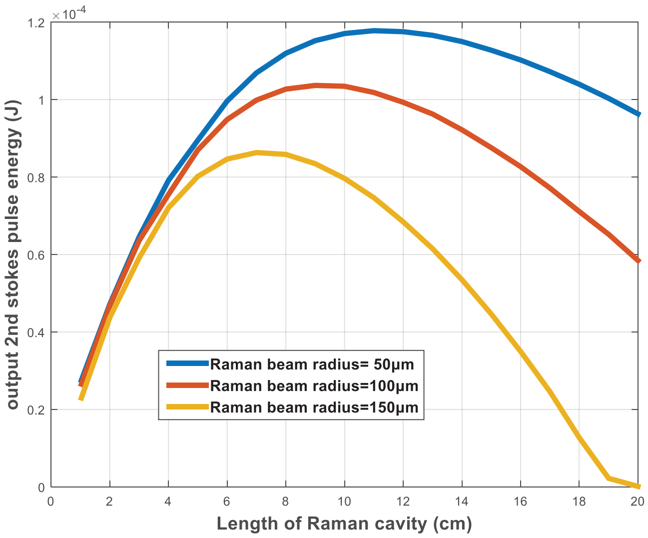

Figure 5. The variation of pulse energy with the cavity length.

the gain medium and Raman crystal are redistributed. Figure 6 shows the pulse shape of the intracavity fundamental photons, intracavity 1st Stokes and output 2nd Stokes at different transmission of insert coupler. When the transmission of the insert coupler mirror is low, major fundamental photons remain in the gain medium, the stimulated emission will be strong. But, as shown in figure 7, the threshold of Stokes generation is high. In contrast, if a high transmission coupler was inserted, more fundamental photons will stay in Raman crystal and first order Raman conversion will be stronger, the threshold of Stokes generation will be decreased. But, because the intensity of stimulated emission becomes weaker, the slope coefficient of Stokes becomes lower.

Therefore, according to figure 8, high transmission coupler should be chosen when pump power is low, and the low transmission one for high pump power. That is to say, we can balance the stimulated emission rate with the first order Raman convert rate by optimizing the transmission of the insert coupler at fundamental laser wavelength.

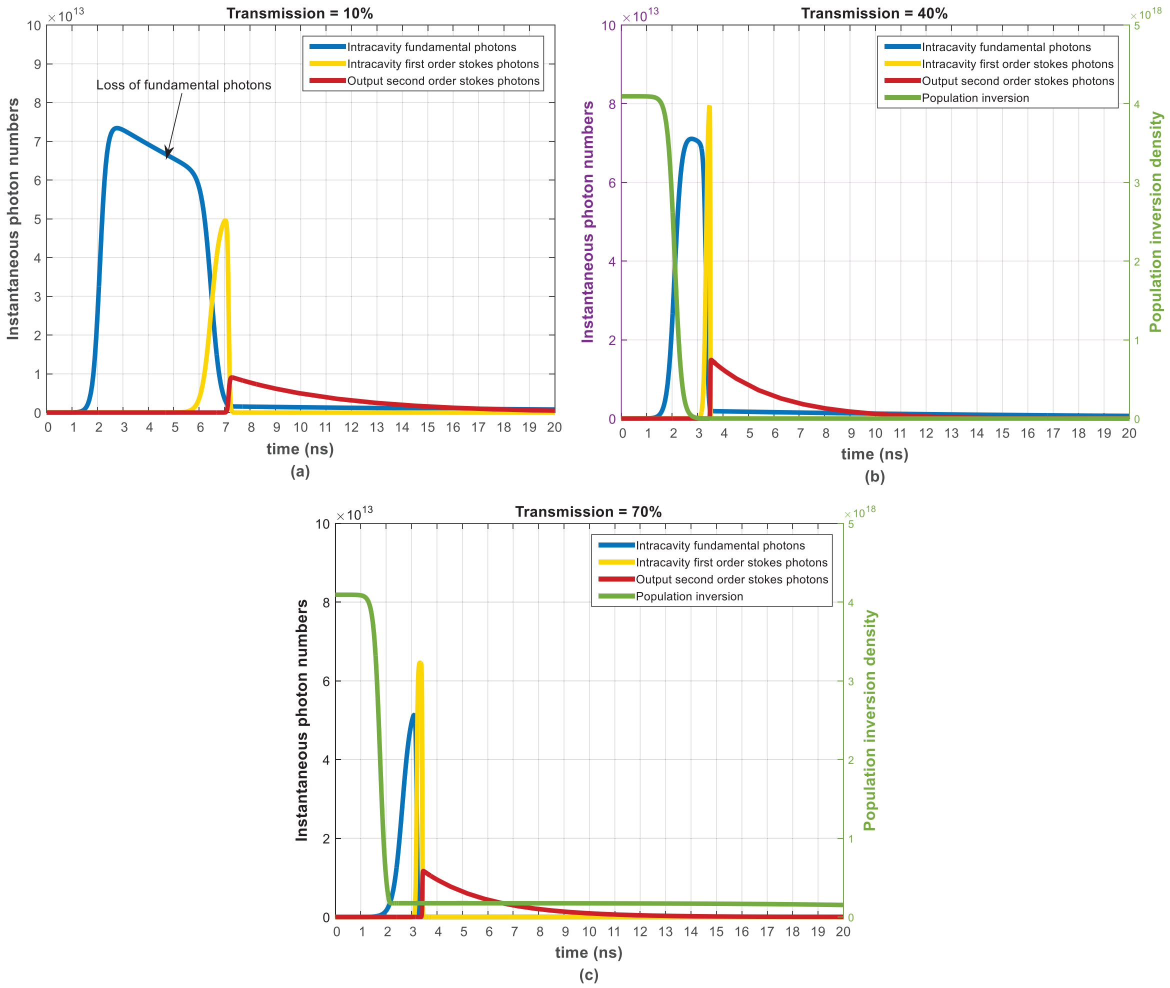

Figure 6. Pulse shape of intracavity fundamental photons, intracavity 1st Stokes and output 2nd Stokes at different transmission of the insert coupler: (a) $T = 10\%$; (b) $T = 40\%$; (c) $T = 70\%$.

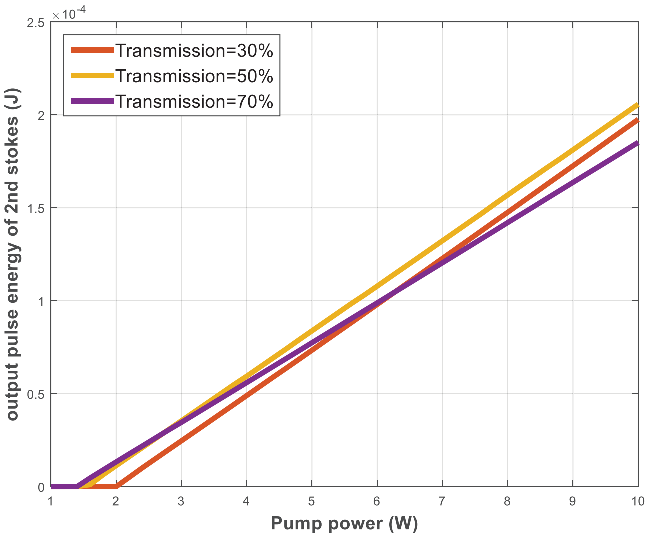

Figure 7. The variation of pulse energy with the pump power at different insert coupling (transmission at fundamental laser wavelength of insert coupler).

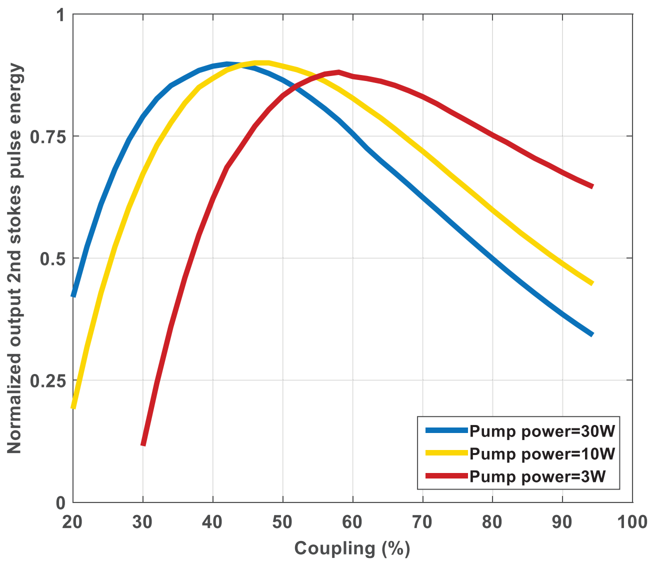

Figure 8. The variation of normalized pulse energy with the insert coupling at different pump powers.

4. Conclusion

In this paper, the model of the intracavity Q-switched second order Raman laser was established, and 2nd Stokes output characteristics were simulated. The dynamic balance mechanism among intracavity convert rates of stimulated emission, first order Raman and second order Raman was obtained for the first time, as far as we know.

Numerical analysis demonstrates that intracavity Stokes photon density can be optimized by adjusting Stokes beam radius, this method is applied to balance the conversion rates between first order and second order Raman scattering. Round trip time of fundamental photons and Stokes photons can be optimized by adjusting Raman cavity length. Additionally, coupled cavity can be applied to redistribute fundamental photons. These last two approaches are useful for balancing convert rates between stimulated emission and first order Raman scatter.

Notwithstanding that the conclusion needs to be verified by further experiment, the results are effective instructions for designing an intracavity Q-switched second order Raman laser for high energy pulse generation.

Acknowledgments

Supported by National Natural Science foundation of China (61405190), National Science and Technology Major Project of China (2014GX04001151); Jilin Scientific and Technological Development Program (20150101041JC, 20160204073GX)

References

[1] Sabella A, Piper J A and Mildren R P 2011 *Opt. Express* **19** 23554–60
[2] Mildren R P, Butler J E and Rabeau J R 2008 *Opt. Express* **16** 18950–5
[3] Parrotta D C, Kemp A J, Dawson M D and Hastie J E 2011 *Opt. Express* **19** 24165–70
[4] Schlosser P J, Parrotta D C, Savitski V G, Kemp A J and Hastie J E 2015 *Opt. Express* **23** 8454–61
[5] Savitski V *et al* 2011 Multi-watt continuous-wave diamond Raman laser at 1217 nm *IEEE Lasers and Electro-Optics Europe* p 1
[6] Chen W, Wei Y, Huang C, Wang X, Shen H, Zhai S, Xu S, Li B, Chen Z and Zhang G 2012 *Opt. Lett.* **37** 1968–70
[7] Du C, Guo Y, Yu Y, Huang G and Ruan S 2013 *Laser Phys. Lett.* **10** 055802
[8] Zhao J, Zhang X, Guo X, Bao X, Li L and Cui J 2013 *Opt. Lett.* **38** 1206–8
[9] McKay A, Liu H, Kitzler O and Mildren R P 2013 *Laser Phys. Lett.* **10** 105801
[10] Demidovicha A A, Voitikovb S V, Batayb L E, Grabtchikovb A S, Danailovc M B, Lisinetskiib V A, Kuzmind A N and Orlovichb V A 2006 *Opt. Commun.* **263** 52–9
[11] Yu X, Pan H, Yan R P, Li X.D, Ma Y F and Gao J 2015 *Opt.-Int. J. Light Electron Opt.* **126** 1282–6
[12] Yashkir Y M 2004 *Proc. SPIE* **5460** 220–7
[13] Zhu F, Gong K and Huo Y 2012 *Opt. Commun.* **285** 2128–33
[14] Spence D J 2015 *IEEE J. Sel. Top. Quantum Electron* **21** 1400108
[15] Dashkevicha V I, Shpaka P V, Voitikova S V, Chulkova R V, Grabtchikova A S, Cheshevc E A, El-Desoukid M and Orlovicha V A 2015 *Opt. Commun.* **351** 1–8
[16] Sabella A, Piper J and Mildren R P 2011 *Conf. on Lasers and Electro-Optics/Pacific Rim* p C725
[17] Mildren R P, Sabella A, Kitzler O, Spence D J and McKay A M 2013 *Optical Engineering of Diamond* (New York: Wiley) pp 239–76
[18] Demidovich A A *et al* 2003 *Appl. Phys.* B **76** 509–14
[19] Zhang X, Zhao S, Wang Q, Ozygus B and Weber H 1999 *IEEE J. Quantum Electron.* **35** 1912–8
[20] Degnan J J 1989 *IEEE J. Quantum Electron.* **25** 214–20
[21] Tucker A W, Birnbaum M, Fincher C L and Erler J W 1977 *J. Appl. Phys.* **48** 4907–11
[22] Savitski V G, Reilly S and Kemp A J 2013 Steady-state Raman gain in diamond as a function of pump wavelength *IEEE J. Quantum Electron.* **49** 218–23